Perturbation Solution for the Flat Spin Recovery of a Dual-Spin Spacecraft

Jean R. Gebman*
The Rand Corporation, Santa Monica, Calif.
and
D. Lewis Mingori†
University of California, Los Angeles, Calif.

Euler's differential equations for free-body attitude motion are solved for the constant bearing axis torque recovery maneuver of a spacecraft with a symmetric rotor and asymmetric platform. The rotor bearing axis coincides with the spacecraft's centroidal principal axis of least inertia. The recovery time and the residual nutation angle are algebraically related to the initial flat spin rate, the spacecraft inertia properties, and the bearing axis torque. The differential equations are solved by use of two asymptotic parameter expansions of the multiple time scale type, which are matched to a transition expansion with a limit process matching procedure.

Introduction

IF the torque motor designed to maintain a specified relative spin rate between the rotor and platform of a dual-spin spacecraft fails to operate, the friction from the rotor bearings will cause the relative spin rate to approach zero. Although the spacecraft angular momentum vector must remain constant, the unavoidable dissipation of energy will cause the spacecraft to seek a minimum energy state of rotation as a unit about the centroidal principal axis of greatest inertia as depicted in Fig. 1.[1-4] Since the least inertia axis coincides with the rotor bearing axis for the spacecraft considered here, such a disabled spacecraft will tumble in a plane perpendicular to the angular momentum vector. This tumbling motion is referred to as a flat spin. If the platform is asymmetrical and the torque motor malfunction is only temporary, the spacecraft can be restored to normal operation by restarting the torque motor and maintaining a small level of torque in excess of that which is required to counteract the bearing friction. As a result, the rotor will spin up relative to the platform and the nutation angle between the rotor bearing axis and the spacecraft angular momentum vector will be reduced from ninety degrees to only a few degrees.[5] While this is happening, the platform spin rate about the bearing axis starts at zero, increases, and then decreases as shown in Fig. 2. When the bearing axis component of the platform rate passes through zero the second time, the motor torque is reduced to exactly counteract the bearing friction. At this time, the spacecraft has reacquired the desired relative spin between the rotor and the platform and the platform is essentially motionless, except for a small residual nutation of the entire spacecraft about the angular momentum vector. In practice, this wobble is removed by a nutation damper, but this aspect of the recovery is not treated here.

The objective of this paper is to represent this recovery process by an asymptotic solution to the governing differential equations of attitude motion. This perturbation solution is used to show that the recovery time is inversely proportional to the torque, whereas the residual nutation angle $[\tilde{\eta}(T_f)]$ is related to the recovery time (T_f) by the flat spin recovery rule

$$G=\Omega\, T_f \tilde{\eta}^2(T_f) \tag{1}$$

where Ω is the initial flat spin rate and G is a constant dependent upon the spacecraft's inertia properties. The exact form of G will be developed later in the paper. In spite of the substantial analytical effort required to obtain such results, the simple manner in which the result captures the role of each of the pertinent parameters illustrates the powerful ability of asymptotic perturbation methods to deal effectively with

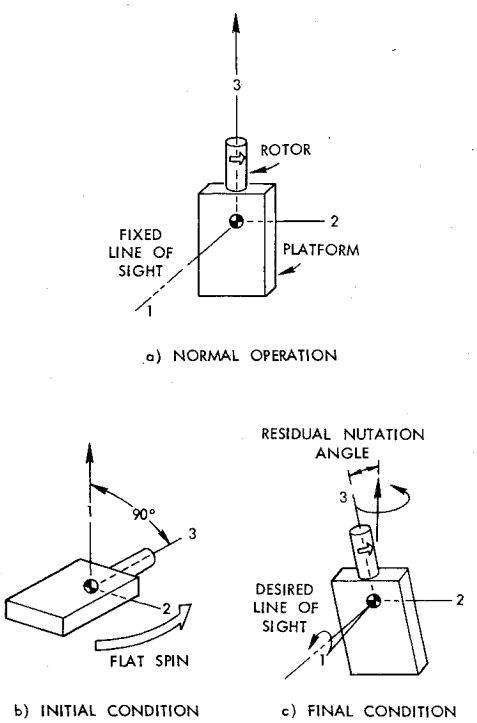

Fig. 1 Illustration of the relevant operating states.

Presented as Paper 75-044 at the AAS/AIAA Astrodynamics Specialist Conference, Nassau, Bahamas, July 28-30, 1975, submitted July 28, 1975; revision received Nov. 17, 1975. The authors wish to than S. Chikwendu, presently at the University of Nigeria at Nsukka, for his assistance in developing the multiple scale expansions, and to specifically acknowledge his suggestion that the dependent variables be represented in two parts, one of which is strictly slowly varying. They also wish to thank J. D. Cole, of the University of California at Los Angeles, for his assistance in developing an approach to the treatment of the transition layer which allowed matching the multiple scale expansions to a transition expansion, and umivkcticular, to acknowledge his recognition of the parameter-free form for the first-order transition layer differential equation and his suggestion of trying a one-time-only numerical integration of this differential equation.

Index categories: Spacecraft Attitude Dynamics and Control, Spacecraft Configurational and Structural Design (including Loads).

*Engineer. Member AIAA.

†Associate Professor. Associate Fellow AIAA.

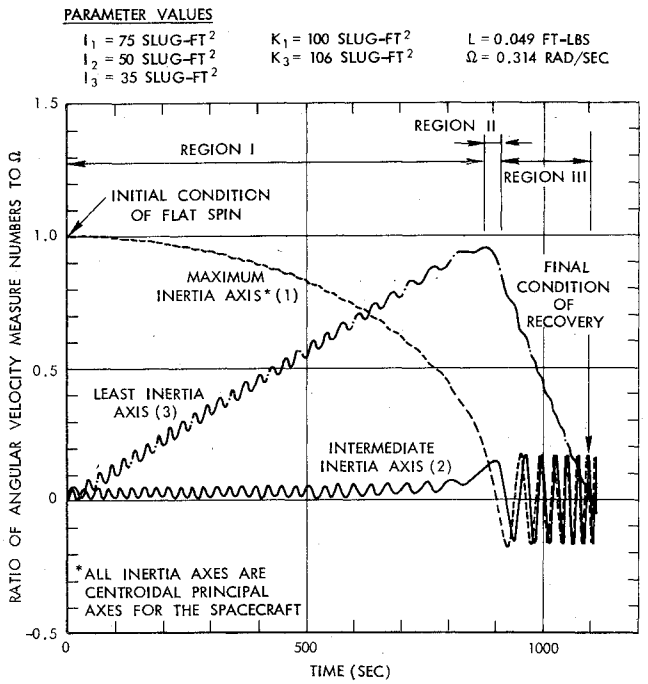

Fig. 2 Platform attitude motion determined by numerical integration of the governing equations of motion for a particular spacecraft design.

complex systems, such as those encountered in the study of spacecraft attitude dynamics. Of particular note is the development of approximate analytical solutions that contribute to the advancement of a general body of knowledge, which may be used to guide the design and operation of future space systems. Previously, the capability of a particular design to recover from a state of flat spin has been studied by numerical integration of the governing equations; a set of coupled, nonlinear, ordinary differential equations. In the present work, the perturbation analysis combines the earlier methods of matched asymptotic expansions with the more recent methods of multiple time scales to treat the three-time intervals of interest. In addition, limit process matching techniques are introduced to allow an intractable parameter-free transition layer differential equation to be numerically integrated. Parameter-free initial conditions are determined by matching with another solution. Since the transition layer differential equation and its initial conditions are free of any parameters, the differential equation must be integrated numerically only once for all possible cases.

Problem Formulation

The system to be studied consists of two freely spinning rigid bodies, whose relative motion is restricted to rotation about a common bearing axis. This axis is the spacecraft's centroidal principal axis of least moment of inertia. It also is the symmetry axis for one body (the rotor) and the centroidal principal axis for both this body and the second asymmetric body (the platform). The relative motion between the rotor and the platform is maintained by a motor, which is used to counteract the bearing friction torque and maintain a desired platform attitude orientation about the bearing axis during normal operation. During the flat spin recovery, this torque is maintained at some constant value (say L) in excess of the bearing friction torque.

Let the spacecraft centroidal principal axes be numbered according to decreasing moments of inertia for the spacecraft (i.e., the 3 axis is the least inertia axis, which is also the bearing axis, etc.), and let I_α and K_α denote the spacecraft centroidal principal moments of inertia for the platform and rotor, respectively; since the rotor is axis-symmetric $K_1 = K_2$. Then the differential equations governing the recovery process may be written as

$$(I_1+K_1)\,(dW_1/dT) - (I_2+K_1-I_3)\,W_2W_3 = -K_3W_sW_2 \tag{2a}$$

$$(I_2+K_1)\,(dW_2/dT) + (I_1+K_1-I_3)\,W_1W_3 = K_3W_sW_1 \tag{2b}$$

$$I_3(dW_3/dT) - (I_1-I_2)\,W_1W_2 = -L \tag{2c}$$

$$K_3(dW_s/dT) = L \tag{2d}$$

where W_α are the components of the platform inertial angular velocity vector projected onto the spacecraft principal axis system, and W_s is the bearing axis component of the rotor inertial angular velocity vector.

The flat spin initial conditions are

$$W_1(0) = \Omega \qquad W_2(0) = W_3(0) = W_s(0) = 0 \tag{3}$$

Subsequent to the initial time, W_3 can be decomposed into a periodic part $\bar{W}_3$ and a nonperiodic part $\tilde{W}_3$. For this discussion, the recovery time T_f is arbitrarily designated as the value of T when the nonperiodic part ($\tilde{W}_3$) becomes zero for the second time, as depicted in Fig. 2:

$$\tilde{W}_3(T_f) = 0 \tag{4}$$

The motivation for this prescription of the recovery time will become evident once the perturbation solution is obtained.

Equations (2-4) can be placed in a form suitable for the perturbation analysis by defining a new set of variables[6]

$$x_1 \triangleq \frac{(I_1+K_1)\,W_1}{(I_1+K_1)\,\Omega} = \frac{W_1}{\Omega} \tag{5a}$$

$$x_2 \triangleq \frac{(I_2+K_1)\,W_2}{(I_1+K_1)\,\Omega} \tag{5b}$$

$$x_3 \triangleq \frac{I_3W_3+K_3W_s}{(I_1+K_1)\,\Omega} \tag{5c}$$

$$s \triangleq \frac{K_3W_s}{\alpha I_3} \tag{5d}$$

$$t \triangleq \alpha\, T \tag{5e}$$

where

$$\alpha \triangleq \left[\left(\frac{I_1+K_1}{I_3}-1\right)\left(\frac{I_1+K_1}{I_2+K_1}-1\right)\right]^{1/2}\Omega \tag{6}$$

It is of interest to note that x_1, x_2, and x_3 represent the normalized components of the angular momentum vector for the spacecraft principal axes; thus

$$x_1^2+x_2^2+x_3^2 = 1 \tag{7a}$$

must be a first integral of Eqs. (2) when they are rewritten in the form

$$\frac{dx_1}{dt} - \frac{1-\lambda^2}{\lambda}x_3x_2 + \epsilon t x_2 = 0 \tag{7b}$$

$$\frac{dx_2}{dt} + \frac{1}{\lambda}x_3x_1 - \epsilon t x_1 = 0 \tag{7c}$$

$$\frac{dx_3}{dt} - \lambda x_1x_2 = 0 \tag{7d}$$

$$s = \epsilon t \tag{7e}$$

with

$$\lambda \triangleq \left\{ \frac{[(I_1+K_1)/(I_2+K_1)]-1}{[(I_1+K_1)/I_3]-1} \right\}^{1/2} \tag{8a}$$

$$\epsilon \triangleq \frac{L}{(I_1+K_1-I_3)[(I_1+K_1)/(I_2+K_1)-1]\Omega^2} \tag{8b}$$

where ϵ is the appropriate smallness parameter for the asymptotic perturbation analysis. The initial conditions, Eq. (3), then become

$$x_1(0)=1 \tag{9a}$$

$$x_2(0)=0 \tag{9b}$$

$$x_3(0)=0 \tag{9c}$$

and the normalized form for the final time specification is obtained from Eqs. (4, 5c, and 7e), by defining $\bar{x}_3(t_f)$ as the nonperiodic part of x_3, whereupon the final recovery time condition becomes

$$\bar{x}_3(t_f) - \epsilon \frac{\alpha}{\Omega}\left(\frac{I_3}{I_1+K_1}\right) t_f = 0 \tag{10}$$

Perturbation Solution

Construction of an asymptotic solution[7,8] for the governing differential equations requires separate consideration of the system's behavior in each of the three regions indicated in Fig. 2. In the first region, a straightforward expansion is used to establish the order of magnitude of the oscillation in region I. Because this expansion fails to capture the slowly varying frequency and amplitude of oscillation characteristic of this region, a multiple scale expansion then is used to include these features of the behavior. Next, the transition region (region II) is considered. Here it is found that a straightforward expansion is adequate after the time scale is stretched. In region III, another multiple scale expansion is developed to again capture the slowly varying amplitude and frequency of oscillation for region III. Space limitations have made it necessary to sharply attenuate any discussion of the procedures for developing the various expansions. Additional details concerning these procedures may be found in Refs. 6-8.

Region I

The system behavior in this region is dominated by the coupled oscillation between x_2 and x_3. The order of magnitude of the oscillation is established by considering a straightforward asymptotic expansion

$$x_i(t;\epsilon) = \sum_{j=1}^{\infty} \mu_{ij}(\epsilon)\, u_{ij}(t); \qquad i=1, 2, 3 \tag{11}$$

which yields the initially valid asymptotic solutions

$$x_1(t;\epsilon) = 1 + 0(\epsilon) \tag{12a}$$

$$x_2(t;\epsilon) = \epsilon - \epsilon\cos t + 0(\epsilon^2) \tag{12b}$$

$$x_3(t;\epsilon) = \epsilon\lambda t - \epsilon\lambda \sin t + 0(\epsilon^2) \tag{12c}$$

Equations (12) correctly indicate the relative sizes of the variables of interest, but they fail to provide adequately for the slowly varying drift of x_1 and x_2 and the slowly varying oscillation frequency and oscillation amplitude for x_2 and x_3, even after considering higher order terms. These features are captured by considering a two-scale representation

$$x_i(t;\epsilon) = \epsilon^{\delta_{i2}} z_i(\tilde{t}) + \sum_{j=1}^{\infty} \mu_{ij}(\epsilon)\, u_{ij}(t^*, \tilde{t}) \qquad i=1, 2, 3 \tag{13}$$

where δ_{i2} is the Kronecker delta function, $\tilde{t}$ is the "slow" time scale, and t^* is the "fast" time scale. As suggested by the initially valid solution, choose

$$\mu_{il}(\epsilon) = \epsilon \qquad i=1, 2, 3 \tag{14a}$$

$$\tilde{t} \triangleq \epsilon\lambda t \tag{14b}$$

and write the governing equation for t^* as

$$dt^*/dt = \psi(\tilde{t}) \tag{14c}$$

where the slowly varying function $\psi(\tilde{t})$ is to be determined by imposing the condition that the oscillations be of constant frequency on the t^* scale. By use of the two-scale representation of Eq. (13), and following the usual multiple scales procedure,[6-8] the region I asymptotic solution becomes

$$x_1^1(t;\epsilon) = (1-\tilde{t}^2)^{1/2} + \epsilon\lambda\tilde{t}(1-\tilde{t}^2)^{-1/4}\sin t^* + 0(\epsilon^2) \tag{15a}$$

$$x_2^1(t;\epsilon) = \epsilon(1-\tilde{t}^2)^{-1/4} - \epsilon(1-\tilde{t}^2)^{1/4}\cos t^* + 0(\epsilon^2) \tag{15b}$$

$$x_3^1(t;\epsilon) = \tilde{t} - \epsilon\lambda(1-\tilde{t}^2)^{1/4}\sin t^* + 0(\epsilon^2) \tag{15c}$$

where

$$t^* = \left\{ \tfrac{1}{2}(1-\tilde{t}^2)^{1/2} + \frac{\sin^{-1}\tilde{t}}{2\tilde{t}} \right\} t \tag{15d}$$

$$\tilde{t} = \epsilon\lambda t \tag{15e}$$

The leading term of the initially valid solution for x_3 [Eq. (12c)] becomes disordered for times $t > 1/\epsilon$, where λ is an 0(1) parameter. Thus, Eqs. (12) are said to be valid initally only for $t << 1/\epsilon$. The two-scale solution [Eqs. (15)] are also valid only in a limited region (termed region I) because of the singularity at $\tilde{t}=1$. The region containing this singularity termed region II) is considered next.

Region II

The coupling of the dominant oscillation changes from x_2 and x_3 (region I) to x_1 and x_2 (region II) in the neighborhood of the singularity ($\tilde{t}=1$) in the region I asymptotic solution. Region II thus is considered to be a thin transition layer in the neighborhood of the singularity $\tilde{t}=1$. An inner expansion, valid in this layer, may be obtained by use of the stretched time scale $\hat{t}$

$$\hat{t} \triangleq (\tilde{t}-1)/\delta(\epsilon) \tag{16}$$

together with a straightforward asymptotic expansion of the form

$$x_i(t;\epsilon) = \delta_{i3} + \sum_{j=0}^{\infty} \mu_{ij}(\epsilon)\, u_{ij}(\hat{t}) \qquad i=1, 2, 3 \tag{17}$$

as suggested by the region I asymptotic solution. Substitution of Eq. (17) into Eqs. (7) leads to a distinguished limit with

$$\mu_{10}(\epsilon) = \epsilon^{1/3} \tag{18a}$$

$$\mu_{20}(\epsilon) = \mu_{30}(\epsilon) = \delta(\epsilon) = \epsilon^{2/3} \tag{18b}$$

and the first set of approximate differential equations, which may be recast in the form

$$\lambda^2 \frac{d^2 u_{10}}{d\hat{t}^2} + (\tfrac{1}{2}u_{10}^2 + \hat{t} + c)u_{10} = 0 \tag{19a}$$

$$u_{20} = -(du_{10}/d\hat{t}) \tag{19b}$$

$$u_{30} = -c - \tfrac{1}{2}u_{10}^2 \tag{19c}$$

where c is an integration constant to be determined from matching. The transition equations [Eqs. (19)], may be put into a parameter-free form with the change of variables

$$y \triangleq \lambda^{-1/3} u_{10} \tag{20a}$$

$$\tau \triangleq \frac{\hat{t} + c}{\lambda^{2/3}} \tag{20b}$$

from which

$$\frac{d^2y}{d\tau^2} + \tfrac{1}{2} y^3 + \tau y = 0 \tag{20c}$$

Before numerically integrating Eq. (20c), the asymptotic initial condition must be determined by matching the asymptotic behavior of the appropriate branch of the solution of Eq. (20c) to the asymptotic behavior of the region I expansion. For this purpose, the asymptotic expansion [Eq. (17)] is written in terms of the new variables y and τ, using Eqs. (18, 19b, 19c, 20a, and 20b):

$$x_1^{II} = \epsilon^{1/3}\lambda^{1/3} y + 0[\mu_{11}(\epsilon)] \tag{21a}$$

$$x_2^{II} = -\epsilon^{2/3}\lambda^{-1/3}(dy/d\tau) + 0[\mu_{21}(\epsilon)] \tag{21b}$$

$$x_3^{II} = 1 - \epsilon^{2/3} c - \epsilon^{2/3}\lambda^{2/3}\tfrac{1}{2} y^2 + 0[\mu_{31}(\epsilon)] \tag{21c}$$

Matching to order $\zeta(e)$ requires[7,9]

$$\lim_{\substack{\epsilon\to 0 \\ t_\eta \text{ fixed}}} (\underline{x}^{Ir} - \underline{x}^{II\ell})/\zeta(\epsilon) = 0 \tag{22a}$$

where $\zeta(\epsilon)$ is an arbitary function of ϵ,

$$t_\eta \triangleq (\tilde{t} - 1)/\eta(\epsilon) \tag{22b}$$

$$1 >> \eta(\epsilon) >> \epsilon^{2/3} \tag{22c}$$

and $\underline{x}^{Ir}$ and $\underline{x}^{II\ell}$ are simply $\underline{x}^{I}$ and $\underline{x}^{II}$ expressed in terms of t_η. When Eqs. (15, 21, and 22b) are used to formulate $\underline{x}^{Ir}$ and $\underline{x}^{II\ell}$, and the resulting expressions are matched to order one [i.e., $\zeta(e) = 1$] using Eq. (22a), the following limits for the x_1, x_2, x_3 components of $\underline{x}^{Ir} - \underline{x}^{II\ell}$ are obtained (higher-order terms in each limit have been neglected):

$$\lim_{\substack{\epsilon\to 0 \\ t_\eta \text{ fixed}}} \{y - (-\epsilon^{-2/3}\lambda^{-2/3} 2\eta t_\eta)^{1/2}\} = 0 \tag{23a}$$

$$\lim_{\substack{\epsilon\to 0 \\ t_\eta \text{ fixed}}} \{(dy/dt_\eta - \epsilon^{-1/3}\lambda^{-1/3}\eta(-2\eta t_\eta)^{-1/2}\} = 0 \tag{23b}$$

$$\lim_{\substack{\epsilon\to 0 \\ t_\eta \text{ fixed}}} \{y^2 + \epsilon^{-2/3}\lambda^{-2/3} 2\eta t_\eta + 2\lambda^{-2/3} c\} = 0 \tag{23c}$$

Satisfaction of Eqs. (23a) and (23c) requires that $c = 0$.

From Eqs. (16, 18b, 20b, and 22b), one obtains an expression for ηt_η in terms of τ, which is arbitrarily designated as τ^ℓ for the left side of region II, i.e., $t_\eta < 0$,

$$\eta t_\eta = \epsilon^{2/3}\lambda^{2/3}\tau^\ell$$

Incorporation of this expression into Eqs. (23a) and (23b) yields the appropriate initial conditions for matching:

$$y(\tau^\ell) = (-2\tau^\ell)^{1/2} \tag{24a}$$

$$\frac{dy}{d\tau}(\tau^\ell) = -1/(-2\tau^\ell)^{1/2} \tag{24b}$$

subject to $\tau^\ell \to \infty$, since for $t_\eta < 0$ and $\eta(\epsilon) >> \epsilon^{2/3}$

$$\lim_{\substack{\epsilon\to 0 \\ t_\eta \text{ fixed}}} \tau^\ell = \lim_{\substack{\epsilon\to 0 \\ t_\eta \text{ fixed}}} \epsilon^{-2/3}\lambda^{-2/3}\eta t_\eta = -\infty$$

Numerical integration of the transition equation [Eq. (20c)] may now commence with the asymptotic initial conditions, Eqs. (24), and a suitably small value for τ^ℓ (e.g., -1000). First, however, one must determine the form of the expected asymptotic behavior as the solution passes through the transition layer on the right side. To accomplish this, let

$$\underline{x}^{IIr} \triangleq \underline{x}^{IIr}\left(\lim_{\substack{\epsilon\to 0 \\ t_\nu \text{ fixed}}} y[\tau(t_\nu;\epsilon)];\epsilon\right) \tag{25a}$$

where $\underline{x}^{IIr}$ is $\underline{x}^{II}$ expressed in terms of t_ν rather than τ, and

$$t_\nu \triangleq (\tilde{t} - 1)/\nu(\epsilon) \tag{25b}$$

$$1 >> \nu(\epsilon) >> \epsilon^{1/3} \tag{25c}$$

From Eqs. (16,20b, and 25b) τ is expressed in terms of t_ν as

$$\tau^r \triangleq \tau(t_\nu) = \nu t_\nu/\epsilon^{2/3}\lambda^{2/3}$$

Hence,

$$\lim_{\substack{\epsilon\to 0 \\ t_\nu \text{ fixed}}} \tau^r = +\infty; \qquad (t_\nu > 0)$$

Now, to preserve the constancy of momentum [Eq. (7a)], y must remain bounded as $\tau^r \to +\infty$. Thus, for sufficiently large values of τ^r, the middle term in Eq. (20c) will be small as compared to the other terms, and this equation can be approximated by

$$\frac{d^2y}{d\tau^{r2}} + \tau^r y = 0, \qquad (\tau^r \to +\infty)$$

The descending solution for y now may be expressed in terms of the decending Airy functions as $\tau^r \to +\infty$ (Ref. 10)

$$y = a_1 Ai(\tau^r) + a_2 Bi(\tau^r) \tag{26}$$

where a_1 and a_2 are constants. Selection of the descending solution for y is justified by the boundedness imposed by the constancy of momentum relation, Eq. (7a). The asymptotic behavior of Eq. (26) for $\tau^r \to +\infty$ is

$$y = A_0(\tau^r)^{-1/4}\cos\{\tfrac{2}{3}(\tau^r)^{3/2} + \phi_0\} \tag{27}$$

where A_0 and ϕ_0 are constants to be determined from the numerical integration. Thus, one expects the asymptotic behavior of y to be of this form as $\tau^r \to +\infty$ in the transition equation [Eq. (20c)].

Integration of the transition equation [Eq. (20c)] with the asymptotic initial conditions [Eq. (24)], for τ suitably close to $-\infty$, say -1000, proceeds to τ suitably close to $+\infty$, say +250. Fitting Eq. (27) to the numerical results for large τ yields

$$A_0 = 0.939 \qquad \phi_0 = 116^\circ \tag{28}$$

It can be confirmed that Eq. (27) is the asymptotic behavior of a solution to Eq. (20c) for $\tau^r \to +\infty$ by assuming an asymptotic expansion for y,

$$y = y_0 + y_1 + \ldots \lim_{\tau^r \to +\infty} (y_1/y_0) = 0 \tag{29}$$

and demonstrating that, if y_0 is given by Eq. (27), then it

follows from Eqs. (20c, 27, 28, and 29) that

$$y_1 = 0(\tau^{r-7/4})$$

Clearly y_1 decays more rapidly than y_0 [where y_0 is given by Eq. (27)] as $\tau^r \to +\infty$. Then, using Eqs. (17-20, 25, 27, and 28), the asymptotic behavior of the region II solution may be written in terms of t_ν for the right side of region II

$$x_1^{IIr}(t;\epsilon) = \epsilon^{1/2}\lambda^{1/2}\ 0.939(\nu t_\nu)^{-1/4} \cdot\cos\left\{\frac{2}{3\epsilon\lambda}(\nu t_\nu)^{3/2} + 116°\right\} + \ldots \tag{30a}$$

$$x_2^{IIr}(t;\epsilon) = \epsilon^{1/2}\lambda^{-1/2} 0.939(\nu t_\nu)^{1/4} \cdot\sin\left\{\frac{2}{3\epsilon\lambda}(\nu t_\nu)^{3/2} + 116°\right\} + \ldots \tag{30b}$$

$$x_3^{IIr}(t;\epsilon) = 1 - \epsilon\lambda\ 0.220\ (\nu t_\nu)^{-1/2} - \epsilon\lambda\ 0.220\ (\nu t_\nu)^{-1/2} \cdot\cos\left\{\frac{2}{\epsilon\lambda}\tfrac{2}{3}(\nu t_\nu)^{3/2} + 232°\right\} + \ldots \tag{30c}$$

This asymptotic behavior of the region II solution will be used to match the asymptotic behavior of the region III solution. The transition region solution is given by Eqs. (17, 18, and 20), with y having been determined by numerical integration of Eq. (20c) for the asymptotic initial conditions [Eqs. (24)]. In theory, one could tabulate the function y for future reference. However, for our purposes, the primary role of the transition solution is to provide an asymptotic expansion [Eqs. (30)] for use in matching the region II and region III solutions. (Note that the transition region is only of $0(\epsilon^{2/3})$ on the $\tilde{t}$ scale. This can be seen from Eqs. (16) and (18b) by requiring that $\hat{t}$ be of 0(1) in the transition region.)

Region III

The final recovery time condition [Eq. (10)] cannot be satisfied, for the general case, either by the region II expansion, Eqs. (21), or its asymptotic behavior, Eqs. (30). Therefore, there must exist a region III to the right of region II, as illustrated in Fig. 2. The asymptotic solution for this new region (say $\underline{x}^{III}$) must have an asymptotic behavior on the left side that agrees with the right-hand side asymptotic behavior of the region II solution. One expects the region III solution to start with a coupled oscillation, between x_1 and x_2, of order $\epsilon^{1/2}$ [see Eqs. (30a) and (30b)]. Figure 2 indicates that the region III solution may involve a slowly varying frequency and amplitude. Thus, it is reasonable to try a two-scale representation

$$x_i(t;\epsilon) = \delta_{i3} + \sum_{j=1}^{\infty} \mu_{ij}(\epsilon)\, u_{ij}(t^*, \tilde{t}) \qquad i = 1,2,3 \tag{31a}$$

with

$$\mu_{11}(\epsilon) = \mu_{21}(\epsilon) = \epsilon^{1/2} \qquad \mu_{31}(\epsilon) = \epsilon \tag{31b}$$

as suggested by $\underline{x}^{IIr}$, Eqs. (30). The slow and fast time scales are given by

$$\tilde{t} \triangleq \epsilon\lambda t \tag{32a}$$

and

$$dt^*/dt = \psi(\tilde{t}) \tag{32b}$$

respectively. The slowly varying function $\psi(\tilde{t})$ is determined by imposing the requirement that the oscillation be of constant frequency on the t^* scale. Proceeding in the usual multiple scales manner[7,8] (intermediate details may be found in Ref. 6), the region III asymptotic solution becomes

$$x_1^{III}(t;\epsilon) = -\epsilon^{1/2}\bar{A}_0(\Gamma_1/\Gamma_2)^{1/4}\cos\{t^* + \phi(\tilde{t})\} + 0(\epsilon^{3/2}) \tag{33a}$$

$$x_2^{III}(t;\epsilon) = -\epsilon^{1/2}\bar{A}_0(\Gamma_2/\Gamma_1)^{1/4}\sin\{t^* + \phi(\tilde{t})\} + 0(\epsilon^{3/2}) \tag{33b}$$

$$x_3^{III}(t;\epsilon) = 1 - \epsilon\frac{\bar{A}_0^2(\Gamma_1+\Gamma_2)}{4(\Gamma_1\Gamma_2)^{1/2}} - \epsilon\frac{\bar{A}_0^2\lambda^2}{4(\Gamma_1\Gamma_2)^{1/2}}\cos\{2t^* + 2\phi(\tilde{t})\} + 0(\epsilon^2) \tag{33c}$$

where

$$t^* = \frac{1}{\epsilon\lambda^2}\left\{\frac{1}{2}\left(\Gamma_2 + \frac{\lambda^2}{2}\right)(\Gamma_1\Gamma_2)^{1/2} - \frac{\lambda^4}{8}\ln\left[2(\Gamma_1\Gamma_2)^{1/2} + 2\left(\Gamma_2 + \frac{\lambda^2}{2}\right)\right] + c_\omega\right\} \tag{33d}$$

$$\phi(\tilde{t}) = \frac{\bar{A}_0^2}{8\lambda^2}\left[\frac{3}{2}\lambda^2\{\ln\Gamma_2 - (1-\lambda^2)\ln\Gamma_1\} + (4-2\lambda^2)\tilde{t}\right] + c_\phi \tag{33e}$$

$$\Gamma_1(\tilde{t}) = \tilde{t} - 1 + \lambda^2 \tag{33f}$$

$$\Gamma_2(\tilde{t}) = \tilde{t} - 1 \tag{33g}$$

where $\bar{A}_0, c_\phi$ and c_ω are integration constants to be determined by matching the left-hand side asymptotic behavior of $\underline{x}^{III}$ to the right-hand side asymptotic behavior of $\underline{x}^{II}$. The matching condition requires that for matching to order $\zeta(\epsilon)$,

$$\lim_{\substack{\epsilon\to 0 \\ t_\nu \text{fixed}}} \left(\frac{\underline{x}^{IIr} - \underline{x}^{III\ell}}{\zeta(\epsilon)}\right) = 0 \tag{34}$$

where $\underline{x}^{III\ell}$ is simply $\underline{x}^{III}$ expressed in terms of the t_ν variable, which was introduced in Eq. (25).

Rewriting Eqs. (33) in terms of t_ν, it is found that

$$x_1^{III\ell}(t;\epsilon) = \epsilon^{1/2}\lambda^{1/2}\bar{A}_0(\nu t_\nu)^{-1/4}\cos\theta^{III\ell} + \ldots \tag{35a}$$

$$x_2^{III\ell}(t;\epsilon) = \epsilon^{1/2}\lambda^{-1/2}\bar{A}_0(\nu t_\nu)^{1/4}\sin\theta^{III\ell} + \ldots \tag{35b}$$

$$x_3^{III\ell}(t;\epsilon) = 1 - \epsilon\frac{\bar{A}_0^2\lambda}{4}(\nu t_\nu)^{-1/2} - \epsilon\frac{\bar{A}_0^2\lambda}{4}(\nu t_\nu)^{-1/2}\cos 2\theta^{III\ell} + \ldots \tag{35c}$$

$$\theta^{III\ell} = \frac{1}{\epsilon}\left[\frac{2}{3\lambda}(\nu t_\nu)^{3/2} + \frac{c_\omega}{\lambda^2} - \frac{\lambda^2}{8}\ln\lambda^2 + 0(\nu^2)\right] + \frac{\bar{A}_0^2}{4}\left\{2 - \lambda^2 - \frac{3}{4}(1-\lambda^2)\ln\lambda^2\right\} + c_\phi + \frac{\bar{A}_0^2}{16\lambda^2}(5-\lambda^2)\nu t_\nu + \frac{3\bar{A}_0^2}{16}\ln(\nu t_\nu) + 0(\nu^2) + \pi \tag{35d}$$

Then matching of all the terms in Eqs. (35) with corresponding terms in Eqs. (30) yields

$$c_\omega = (\lambda^4/8)\ln\lambda^2 \tag{36a}$$

$$c_\phi = \left(\frac{116°}{180°} - 1\right)\pi - \frac{\bar{A}_0^2}{4}\left\{2 - \lambda^2 - \frac{3}{4}(1-\lambda^2)\ln\lambda^2\right\} \tag{36b}$$

$$\bar{A}_0 = 0.939 \tag{36c}$$

with all of the remaining terms in Eqs. (30) being of higher order than those that were matched. Thus, the matched asymptotic solution for region III is given by Eqs. (33) and (36).

Recovery Rule

The asymptotic solution for region III [Eqs. (33) and (36)] now is used to determine the final recovery time and the flat spin recovery rule [Eq. (1)]. The nonperiodic part of the asymptotic solution for x_3^{III} is, from Eq. (33c),

$$\bar{x}_3(t_f) = 1 - \epsilon 0.440 \frac{\tilde{t}_f - 1 + \tfrac{1}{2}\lambda^2}{[(\tilde{t}_f - 1 + \lambda^2)(\tilde{t}_f - 1)]^{1/2}} + 0(\epsilon^2) \tag{37}$$

Substitution of Eq. (37) into the recovery condition [Eq. (10)] yields

$$1 - \epsilon\left\{0.440 \frac{\tilde{t}_f - 1 + \tfrac{1}{2}\lambda^2}{[(\tilde{t}_f - 1 + \lambda^2)(\tilde{t}_f - 1)]^{1/2}} + \frac{\alpha}{\Omega}\frac{I_3}{I_1 + K_1} t_f\right\} + 0(\epsilon^2) = 0 \tag{38}$$

In order to obtain an approximate expression for the recovery time (t_f), make the change of variables

$$\bar{t} \triangleq \tilde{t}_f - 1 \tag{39a}$$

and expand the new variable in powers of ϵ, say

$$\bar{t} = \bar{t}_0 + \epsilon \bar{t}_1 + 0(\epsilon^2) \tag{39b}$$

Substituting Eqs. (32a) and (39) into Eq. (38), and comparing like powers of ϵ, leads to the results

$$\bar{t}_0 = J - 1 \tag{40a}$$

$$\bar{t}_1 = -0.440 \frac{[J^2 - (1 - \tfrac{1}{2}\lambda^2)J}{[J^2 - 2(1 - \tfrac{1}{2}\lambda^2)J + 1 - \lambda^2]^{1/2}} \tag{40b}$$

where

$$J \triangleq \frac{I_1 + K_1}{I_1 + K_1 - I_3} \tag{40c}$$

Thus, from Eqs. (32a, 39, and 40),

$$t_f = \frac{1}{\epsilon}\left\{\frac{J}{\lambda}\right\} - \left\{\frac{0.440}{\lambda}\left(\frac{J^2 - (1 - \tfrac{1}{2}\lambda^2)J}{[J^2 - 2(1 - \tfrac{1}{2}\lambda^2)J + 1 - \lambda^2]^{1/2}}\right)\right\} + 0(\epsilon) \tag{41}$$

Substitution of Eq. (41) into Eq. (37) yields

$$\bar{x}_3(t_f) = 1 - \epsilon\left[0.440\left\{1 + \tfrac{1}{2}\left(\frac{I_1 - I_2}{I_2 + K_1}\right)\right\}^{1/2}\right] + 0(\epsilon^2) \tag{42}$$

Observe that the nutation angle (η) may be expressed in terms of x_3 as

$$\eta = \sin^{-1}(1 - x_3^2)^{1/2}$$

It is suitable for present purposes to define the residual nutation angle based upon the nonperiodic part of x_3,

$$\bar{\eta}(t_f) \triangleq \sin^{-1}[1 - \bar{x}_3^2(t_f)]^{1/2} \tag{43}$$

Substituting Eq. (42) into Eq. (43) yields

$$\bar{\eta}(t_f) = \epsilon^{1/2}\left[0.939\left\{1 + \tfrac{1}{2}\left(\frac{I_1 - I_2}{I_2 + K_1}\right)\right\}^{1/4}\right] + 0(\epsilon^{3/2}) \tag{44}$$

The flat spin recovery rule [Eq. (1)] then is obtained by combining the leading term in the expansion for t_f, Eq. (41), with Eq. (44) in order to eliminate ϵ from Eq. (44). The resulting expression for G is

$$G = 0.880 \frac{\left[1 + \tfrac{1}{2}\left(\frac{I_1 - I_2}{I_2 + K_1}\right)\right]^{1/2}}{\left(1 - \frac{I_3}{I_1 + K_1}\right)\left(\frac{I_1 - I_2}{I_2 + K_1}\right)} \tag{45}$$

where T_f in Eq. (1) is related to t_f by Eq. (5e)

$$T_f = (1/\alpha)\, t_f \tag{46}$$

and α is defined in Eq. (6).

The required torque level for a given flat spin recovery operation may be determined from Eq. (41) by simplifying that expression with the help of Eqs. (46, 40c, 8, and 6), where for a specified recovery time T_f and initial flat spin rate Ω, the required excess torque level L is given by

$$L = (I_1 + K_1)\Omega / T_f \tag{47}$$

This torque level (in excess of the bearing friction torque) generally will be very small in order to insure that the residual nutation angle is small enough to be completely removed by a nutation damper, which becomes effective only during the final stages of recovery.

Comparison with Numerical Integration Results

For a given spacecraft (i.e., values for I_α, K_α) and a set of operating conditions (i.e., values for Ω and L), one may compute the approximate time for recovery and the approximate residual nutation angle from Eqs. (1) and (47). Table 1 presents a comparison of such approximate results with the results of numerical integration of the governing differential equations [Eqs. (2)], for 27 cases. The cases have been ordered according to increasing normalized parameter values of ϵ and λ in order to illustrate the impact of the size of ϵ and λ upon the accuracy of the results. The recovery time has been reported in the nondimensional form $T_f\Omega$.

The error in the asymptotic estimate of the recovery time is less than a few percent, provided that $\epsilon < 0.1$ and $\lambda > 0.1$. The error in the asymptotic estimate of the residual nutation angle is less than 10%, provided that $\epsilon < 0.02$ for the indicated range of values for λ. For reasonably small values of ϵ (say $\epsilon < 0.1$) and for $\lambda >> \epsilon$ [recall that we stipulated that λ would be an 0(1) parameter], the percentage errors are within quite acceptable bounds for the purposes of the present analysis. It is of interest to note, however, that the errors do not seem to follow any particular pattern. The data in Table 1 show why this is the case. As an example, consider cases 10 and 11. The percentage error in the asymptotic estimate of the residual nutation angle "jumps" from -11.8 to -1.7% for only a 3% increase in ϵ (the changes in λ and α/Ω are less than 1%). It can be seen from the form of the asymptotic solution [Eq. (44)] that as ϵ increases the residual nutation angle also increases. This generally is the case with the data in Table 1. However, with cases 10 and 11, it is observed that, as the value of ϵ increased by 3%, the residual nutation angle from the numerical solution decreased by 9%. Obviously, the spacecraft motion, as evidenced by the numerical solution, is not completely represented by the leading terms of the asymptotic expansions [e.g., Eq. (44)]. This is to be expected since the asymptotic solution is only as accurate as the number of terms retained. In theory, consideration of higher-order terms would account for some of the observed variability in the results.

The order of the error of the asymptotic estimate of the residual nutation angle can, of course, be estimated from Eq. (44), since the error committed by truncating the asymptotic

Table 1 Comparison of the asymptotic and numerical solutions for the recovery time and the residual nutation angle

Case number	Normalized parameters in the asymptotic solution			Numerical solution		Percent deviation by the asymptotic solution	
	ϵ	λ	α/Ω	Nondimensional recovery time $T_f\Omega$	Residual nutation angle, deg	Recovery time, %	Residual nutation angle, %
1	0.005	0.5	0.5	1596	3.75	0.2	4.5
2	0.005	0.75	0.75	709	4.07	0.2	− 0.5
3	0.00779	0.3385	1.354	349	5.15	0.3	− 2.9
4	0.01	0.25	0.25	3186	5.48	0.3	− 1.0
5	0.01	0.5	0.5	796	5.25	0.3	5.6
6	0.01	0.75	0.75	354	5.50	0.3	4.1
7	0.01014	0.2083	0.8452	695	5.45	0.4	1.5
8	0.01205	0.2722	1.0885	348	6.08	0.5	0.5
9	0.02028	0.2083	0.8452	345	8.42	1.0	− 7.0
10	0.02143	0.2041	0.8166	345	9.11	1.0	−11.8
11	0.022	0.2025	0.8099	343	8.28	0.8	− 1.7
12	0.05002	0.25	0.25	625	12.35	1.8	− 1.8
13	0.04998	0.5	0.5	157	11.25	1.7	10.2
14	0.05	0.75	0.1876	688	14.58	2.8	−16.1
15	0.10004	0.25	0.25	302	19.39	4.7	−11.5
16	0.10003	0.3	0.3	212	17.27	3.6	− 0.4
17	0.10001	0.4	0.4	120	16.79	3.1	3.3
18	0.1	0.5	0.5	73	22.90	7.7	−23.5
19	0.09999	0.6	0.6	54	16.19	2.5	9.5
20	0.1	0.7	0.7	39	18.66	3.4	− 3.7
21	0.1	0.75	0.75	33	21.88	7.2	−17.3
22	0.10178	0.093	0.3774	319	23.77	8.3	−27.5
23	0.10968	0.0616	0.4774	320	23.75	7.9	−24.7
24	0.12143	0.0858	0.343	322	23.18	7.4	−18.8
25	0.13601	0.1085	0.271	306	29.05	12.7	−31.4
26	0.2	0.5	0.5	35	27.26	11.5	− 9.1
27	0.2267	0.198	0.1484	283	36.30	20.7	−29.2

expansion after the first term is numerically of the order of the second term. Thus, the error should be of $0(\epsilon^{3/2})$. This requirement is satisfied in Fig. 3, where the error of the asymptotic estimate of the residual nutation angle is plotted as a function of ϵ for the 27 cases considered in Table 1. Nearly all of the points (89%) lie below the line $5\,\epsilon^{3/2}$, and 78% of the points lie between that line and the line $0.5\,\epsilon^{3/2}$. This demonstrates that the error is growing as $\epsilon^{3/2}$ as expected from Eq. (44).

Example Application

The flat spin recovery rule developed in the preceding can be of significant value for evaluating or modifying a given spacecraft design in order to improve its recovery characteristics. (The term *recovery characteristics* refers to the recovery time and residual nutation angle.) In order to assist in the consideration of specific systems, a graphical representation of the recovery rule will be developed.

The relationship between the recovery characteristics and the ratio G/Ω is displayed in Fig. 4, which is based on Eq. (1). Subsequent discussions will be concerned with values of G/Ω of roughly 3 to 100 sec. Figure 4 shows that the achievement of a residual nutation angle as small as 6° to 10° will require a few minutes to a few hours, in this range of values for G/Ω. Although it would be desirable (from the flat spin recovery point of view) to have a high value for Ω, normal operating conditions are typically such that Ω may be in the neighborhood of 1 to 3 rad/sec. The role of the spacecraft inertia

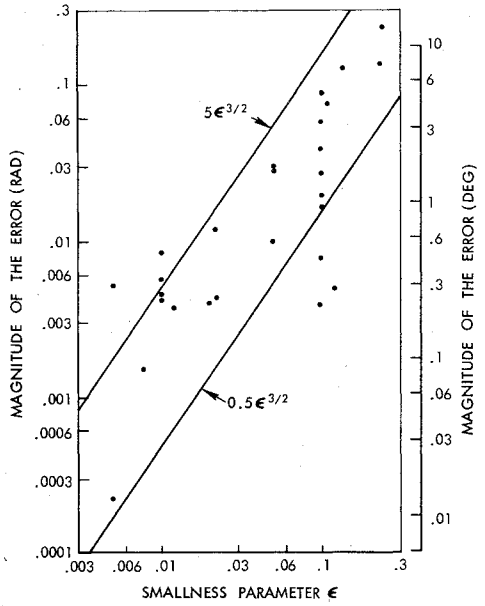

Fig. 3 The ϵ dependency of the error in the asymptotic estimate of the residual nutation angle for the cases in Table 1.

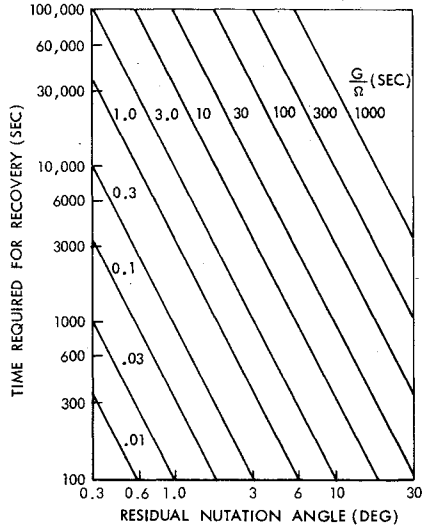

Fig. 4 Tradeoff between the recovery time and the residual nutation angle.

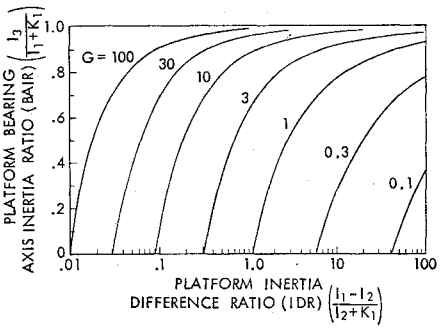

Fig. 5 Dependence of G upon the spacecraft inertia parameters.

properties is rather complicated, and for that reason, Fig. 4 simply summarizes these effects in the form of the G constant. In order to gain a deeper insight into the significance of this constant, the expression for G [Eq. (45)] has been plotted in terms of the two inertia ratios appearing in Eq. (45) (Fig. 5). For convenience, the following terms will be used to refer to these ratios

$$\frac{I_3}{I_1+K_1} = \text{Platform Bearing Axis Inertia Ratio} = \text{BAIR}$$

$$\frac{I_1-I_2}{I_2+K_1} = \text{Platform Inertia Difference Ratio} = \text{IDR}$$

Figure 5 shows that the value of G increases quite rapidly for values of the platform BAIR in the range of 0.8 to 1. Note that the BAIR must be greater than zero and less than 1 according to axis convention. The only restriction on the value for the platform IDR is that it must be greater than zero. Since the IDR takes on such a wide range of values, and has such a substantial impact on the value of G, the dependence of the IDR upon the spacecraft's inertia properties will be considered next (Fig. 6).

Figure 6 shows that the value of the IDR decreases quite rapidly for values of the transverse inertia ratio (I_2/I_1) in the range of 0.8 to 1.0. Note that the transverse inertia ratio (I_2/I_1) must remain less than one. The only restriction on the rotor inertia ratio (K_1/I_1) is that it must be greater than zero. If the transverse inertia ratio (I_2/I_1) is in the neighborhood of 0.6 or less, the rotor inertia ratio (K_1/I_1) exercises considerable influence over the value of the IDR.

Figure 4 shows that, in order to achieve more favorable recovery characteristics, it is desirable to reduce the value of G. If the value for the BAIR (Fig. 5) is already less than 0.8, then the most effective way to do this is to increase the IDR (Fig. 5). In addition, if the value for the transverse inertia ratio (I_2/I_1) is less than 0.6, then the most leverage is obtained by reducing the mass of the rotor (i.e., the rotor inertia ratio K_1/I_1 – see Fig. 6).

The foregoing discussion has considered the algebraic dependence of G upon the inertia properties (I_1,I_2,I_3,K_1). There are, however, certain constraints that the inertia properties must satisfy. These constraints result in certain limitations (which are not apparent in Fig. 5) on the possible value of G. First, by the axis convention,

$$I_1 > I_2 \tag{48a}$$

$$I_2+K_1 > I_3+K_3 \tag{48b}$$

In addition, the sum of the inertias for any two principal axes must be greater than, or equal to, the inertia for the third principal axis. Thus, for the platform

$$I_1+I_2 \geq I_3 \tag{48c}$$

$$I_2+I_3 \geq I_1 \tag{48d}$$

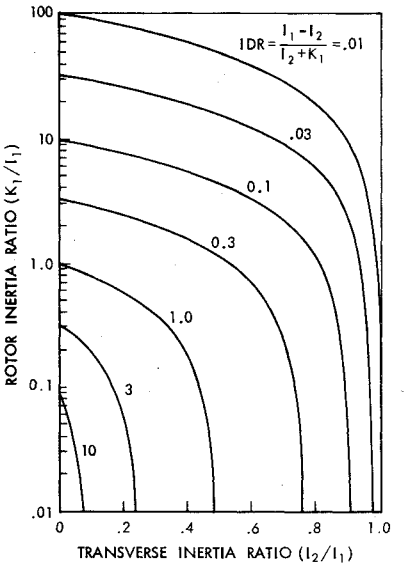

Fig. 6 Dependence of the inertial difference ratio (IDR) on the spacecraft's inertia properties.

$$I_3+I_1 \geq I_2 \tag{48e}$$

and the rotor

$$2K_1 \geq K_3 \tag{48f}$$

and for the overall spacecraft

$$I_1+I_2+2K_1 \geq I_3+K_3 \tag{48g}$$

$$I_2+I_3+K_3 \geq I_1 \tag{48h}$$

$$I_3+K_3+I_1 \geq I_2 \tag{48i}$$

Figure 7 incorporates these constraints in presenting the possible range of values for G as a function of the allowable values for I_3/I_1 and I_2/I_1 for selected values of K_1/I_1 and K_3/I_1. For example, if $K_1/I_1 = 1.0$ and $K_3/I_1 = 1.0$, then all possible values of I_2/I_1 and I_3/I_1 lie within the triangle ABC in Fig. 7. The resulting values of G range from 4 to over 100. The right-most limiting line (or placard) is given by Eq. (48a). The lower left placard comes from Eq. (48d). The upper left placard comes from Eq. (48b) for the indicated values of K_3/I_1. The noted constraint on K_3/I_1 comes from Eq. (48f). Equation (48c), 48e, and 48g-48i) are constraints that are weaker than the aforementioned placards. As an example, consider a hypothetical spacecraft in a flat spin with

$$\Omega = 3.5 \text{ rad/sec}$$

and the following principal inertia properties

$$I_1 = 475 \text{ slug-ft}^2 \quad K_1 = 525 \text{ slug-ft}^2$$

$$I_2 = 465 \text{ slug-ft}^2 \quad K_2 = 525 \text{ slug-ft}^2$$

$$I_3 = 160 \text{ slug-ft}^2 \quad K_3 = 500 \text{ slug-ft}^2$$

relative to the spacecraft center of mass. Then

$$K_1/I_1 = 1.1 \qquad I_2/I_1 = 0.98$$

$$\text{IDR} = (I_1-I_2)/(I_2+K_1) = 0.01$$

$$\text{BAIR} = I_3/(I_1+K_1) = 0.16$$

and from Eq. (45)

$$G/\Omega = 30 \text{ sec}$$

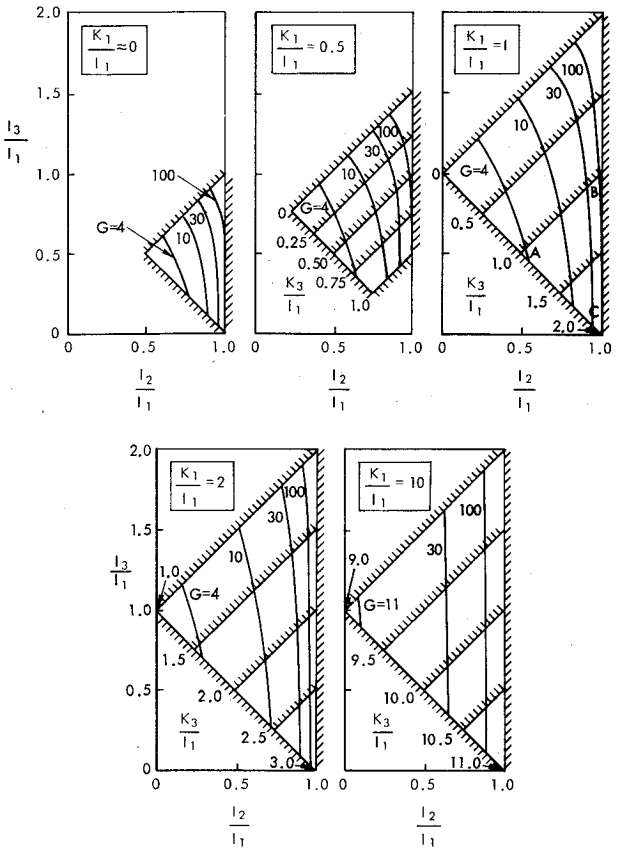

Fig. 7 Dependence of G upon the spacecraft inertia properties.

Assume that the flat spin recovery characteristics associated with a G/Ω of 30 sec (see Fig. 4) are unsatisfactory. Furthermore, assume that the value of Ω (already 3.5 rad/sec) cannot be increased. Now determine what changes would lead to a spacecraft design with a G/Ω of 3 sec. (Such an improvement would result in a tenfold reduction in the recovery time for a given residual nutation angle.)

Turning to Fig. 5 and noting the location of the point (IDR = 0.01, BAIR = 0.16) for this hypothetical design, one sees that there is a very little benefit to be achieved by decreasing the BAIR. Thus, a tenfold reduction in G requires an increase in the IDR from 0.01 to about 0.1. Considering Fig. 6 and noting the location of the point

$$(I_2/I_1 = 0.98 \qquad K_1/I_1 = 1.1)$$

for this hypothetical spacecraft design, it is clear that the most leverage is obtained by reducing I_2/I_1. In particular, a reduction of I_2/I_1 from 0.98 to about 0.81 would achieve the desired tenfold increase in the IDR, and thus the required tenfold increase in G. Of course, the indicated reduction in I_2/I_1 might not prove to be practical when other constraints on the design of the hypothetical spacecraft are considered. However, inspection of Fig. 7 for $K_1/I_1 = 1.1$, $I_3/I_1 = 0.34$, and $I_2/I_1 = 0.81$ shows that such a set of values describes a physically possible spacecraft [i.e., the inertia constraints of Eqs. (48) are satisfied]. The present purpose, however, only has been to illustrate the application of the flat spin recovery rule to a hypothetical design.

Conclusions

Dynamical analysis of the attitude orientation of even the simplest of dual-spin spacecraft normally leads to a system of highly coupled nonlinear ordinary differential equations, which defy general analytical solution. Sometimes it is possible to identify particular steady-state motions for which exact analytical solutions may be obtained, and in such cases, one may examine the stability of these solutions by linearization or the direct method of Liapunov. Most such analytical studies have treated the unforced or homogeneous problem, in which the rotor is spinning at a constant rate relative to the platform. This paper has treated the more difficult problem of determining the transient response for the forced or nonhomogeneous case, in which the rotor is being accelerated by a constant torque. In this case, the entire spacecraft undergoes large changes in angular orientation. This feature makes it necessary to employ the tools of perturbation analysis, based upon asymptotic parameter expansions instead of the linearization technique often used in stability analysis. The resulting solution of the constant torque two-body problem, for the simple case in which the bearing axis coincides with the centroidal principal axis of least-moment inertia of the system, represents a significant first step in adapting asymptotic perturbation methods to the study of the dynamical behavior of space systems with multiple moving parts.

References

[1] Likins, P. W., "Effects of Energy Dissipation on the Free Body Motions of Spacecraft," Jet Propulsion Laboratory, TR 32-860, July 1, 1966.

[2] Landon, V. D. and Stewart, B., "Nutational Stability of an Axisymmetric Body Containing a Rotor," *Journal of Spacecraft and Rockets*, Vol. 1, Nov.-Dec., 1964, pp. 682-684.

[3] Likins, P. W., "Attitude Stability Criteria for Dual-Spin Spacecraft," *Journal of Spacecraft and Rockets*, Vol. 4, Dec. 1967, pp. 1638-1643.

[4] Mingori, D. L., "Effects of Energy Dissipation on the Attitude Stability of Dual-Spin Satellites," *AIAA Journal*, Vol. 7, Jan. 1969, pp. 20-27.

[5] Velman, J. R. and Belardi, J. W., "Gyrostat Attitude Dynamics," Hughes Aircraft Company, SSD 90154R, May 1969.

[6] Gebman, J. R., *Perturbation Analysis of the Flat Spin Recovery of a Dual-Spin Spacecraft*, Ph.D. dissertation, University of California, Los Angeles, June 1974.

[7] Cole, J. D., *Perturbation Methods in Applied Mathematics*, Blaisdell, Waltham, Mass., 1968.

[8] Nayfeh, A. H., *Perturbation Methods*, Wiley, New York, 1973.

[9] Lagerstrom, P. A. and Casten, R. G., "Basic Concepts Underlying Singular Perturbation Techniques," *SIAM Review*, Vol. 14, Jan. 1972, pp. 63-120.

[10] Abramowitz, M. and Stegun, I. A., eds., *Handbook of Mathematical Functions*, Dover, New York, 1965.